Biogeochemistry of Permafrost Thermokarst Lakes in the Canadian Subarctic

Leandro Castanheira
leandro.castanheira@tecnico.ulisboa.pt

Centro de Química Estrutural, Instituto Superior Técnico, Universidade de Lisboa, Lisboa, Portugal

Abstract

In order to better understand the biogeochemical processes occurring in thermokarst lakes fieldwork was carried out in the Canadian sub-Arctic. Several soils, sediments and waters were sampled in lakes localized in different permafrost areas. To chemically characterize the samples in terms of their composition and trace elements (TEs) content, several analytical techniques were used. In this work sulphur compounds were measured for the first time. The reduction of dissolved oxygen and sulfate with depth in the water column of all lakes, suggested their consumption during the mineralization of the Natural Organic Matter, such as dissolved organic carbon (DOC) which increased with depth apparently related to the molecular diffusing (and/or frozen effect) of DOC at the sediment/water interface. More than 14% of analyzed TEs were remobilized in water when DOC mineralized, which may precipitate by the production of sulphide ions. High sedimentary organic matter was observed in SAS/KWK lakes samples (max. 94%) while in BGR lake samples lowest levels were determined (<2%). Also, organic-S was less abundant in this lake accounting only 33% whereas for the others more than 50% was observed. A tendency for TEs to increase with higher aluminium content in soils/sediments was verified suggesting an association with inorganic material, with sulphides playing an important role. This work points to the importance of the organic matter composition in the biogeochemical processes occurring in thermokarst lakes. To the best of my knowledge, for the first time it was proved the importance of the sulphur chemistry in these carbon-enriched freshwater systems.

Keywords: Canadian sub-arctic, *permafrost*, organic carbon, sulphur, trace elements

1. Introduction

Permafrost is defined as the ground that remains at or below 0ºC for more than two consecutive years [1]. It can be differentiated by its spatial extent into continuous (90-100%), discontinuous (50-90%), sporadic (10-50%), and isolated (0-10%) permafrost [1]. Warming permafrost may be accompanied by releasing of ancient organic carbon, with a positive feedback on carbon cycle

[2]. An increase on climate temperature will likely increase permafrost degradation and reduce its extent [3]. A typical form of permafrost degradation involves the formation and growth of thermokarst lakes, also called, thaw lakes [4].

These lakes are widespread in Arctic and sub-Arctic lowland regions with ice-rich permafrost during the Late Pleistocene-Holocene transition [5]. The general distribution of thermokarst lakes in Alaska, Russia, and Canada is known from a number of regional lake studies and maps in various levels of details [6-8].

Thermokarst lakes have also been identified as an important source for atmospheric greenhouse gases [9]. Anaerobic environments in the these lake's bottom and thawed sediments beneath them result in the microbial decomposition of organic matter and methane production that contribute as northern methane source to the current atmospheric carbon budget [10].

Most of our knowledge of these lakes is mainly related to the microbiological formation, fluxes and release of CO_2 and CH_4 or on less extend the chemical composition of thermokarst soils and waters [11]. Others have dedicated more of their research to the biotic side of these lakes and also to the limnological aspects involved [12]. Low molecular weight from natural organic matter (NOM) has been identified as an important ruler of CO_2 production [13]. The aspect of high stratification of these lakes in the summer because of warmer temperature of surface water, compared to the bottom, was also noted in many papers [14]. Trace elements biogeochemical studies are scarce and mostly published by Pokrovsky group [15] done in Siberia mainly focused in trace element colloidal speciation, chemical composition or microbial activity.

In spite of these works, many scientific gaps still persist in order to understand the geochemical processes of thaw lakes and how their chemistry affect the gas release and microbial activity, mainly related to NOM composition and their relation to trace element speciation, partitioning and transport.

This work presents an initial study of the biogeochemistry of thermokarst lakes. For that we sampled and characterized four lakes on discontinuous and sporadic permafrost of Nunavik, Quebec, Canada region. This work is also a contribution to the thaw permafrost lakes studies since, for the first time, relate the chemical composition of the organic matter in those lakes with their chemistry, and particularly with the biogeochemical processes involving organic matter, and other trace element speciation, partitioning and fate.

2. Study Sites

All samples (waters/sediments/soils) collected between Jun 26th and July 3th 2014, were from three different subarctic valleys: SAS, KWK, and BGR (figure 1).

SAS thaw lakes (55º13N 77º43W) are part of a permafrost peatland, covering approximately 5 km^2 at a mean altitude of 105 m above sea level [17]. The site is located in the sporadic permafrost zone in the Sasapimakwananisikw River located 7 km to the south to the village of *Whapmagoostui-Kuujjuarapik* (W-K) at the edge of Hudson Bay, subarctic Québec, Canada [18]. These thaw lakes are black, highly stratified [19] and originated from palsas (mounds of peat containing a permafrost core of peat or silt) after their collapsing [20].
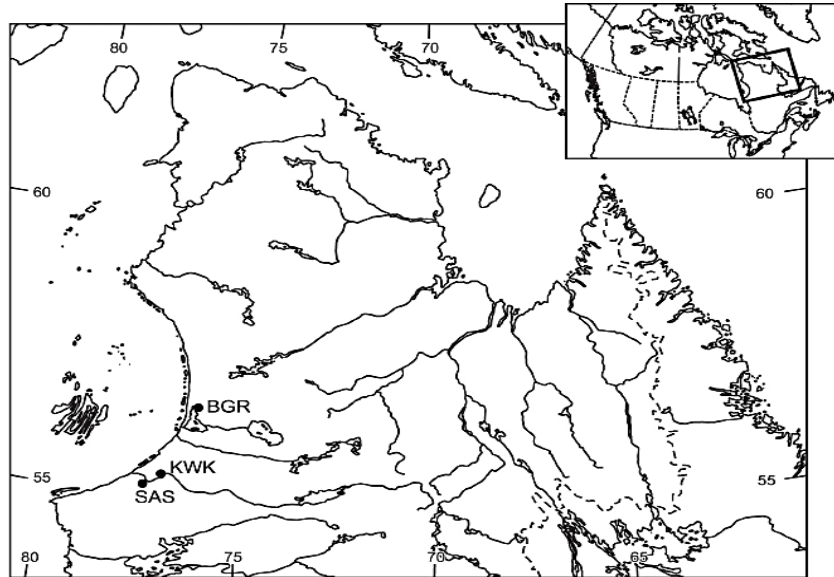
Figure 1: Location of the three sampling valleys in Nunavik, subarctic Québec, Canada. Extracted from Crevecoeur et al. (2015).

The KWK thaw lakes (55º20N 77º30W) lie in a zone of sporadic permafrost in the Kwakwatanikapistikw River valley, 110 m above sea level and 12 km to the east of W-K, spanning a wide range of colors [10]. These lakes derived from fully thawed lithalsas, with extensive tree and shrub development around the lakes [19].

The KWK and SAS lakes are in two separate river valleys close to the village of Whapmagoostui-Kuujjuarapik in the sporadic permafrost zone, while the BGR ponds (56º37´N; 76º13´W) are in the Sheldrake River valley close to the village of Umiujaq, Québec, in the discontinuous permafrost region.

BGR lakes are in the Sheldrake River valley, in the discontinuous permafrost region. These ponds have formed in thawing permafrost mounds that are primarily organic (peat) or mineral [21]. BGR and KWK ponds originated from the thawing of lithalsas and are surrounded by shrubs (*Salix planifolia* and *Betula glandulosa*) and sparse trees (*Picea mariana*, *Picea glauca*, *Larix laricina*) [13].

KWK and BGR lakes originated from the thawing permafrost mounds that are lithalsas and SAS

lakes from palsas; the term palsa refers to organic mounds and lithalsa to mineral mounds [20].

3. Sampling

Before sampling all material was acid decontaminated according to the clean protocol [22]. Vertical profiles of physico-chemical parameters from the sampled thaw ponds were recorded: pH, DO (dissolved oxygen), conductivity and temperature. These parameters were measured with 600R multi-parametric probe (Yellow Spring Instrument).

Water samples were collected at different depths. These depths were previously chosen according to the water profiles using vertical profile of DO as a criterion. Sampled waters were used to determined dissolved trace elements (total and labile), dissolved organic carbon (DOC), dissolved sulphur species (sulfate and sulphide), and for δ^{13}C-DOC analysis. All samples were acidified with 10µL of double distilled HNO_3 in 10 mL polyethylene tubes, after filtered *in situ* with a 0.45 µm pore size acetate filters (Whatman) for sulphur and total trace-element analysis or glass

fiber filter (Whatman) for organic carbon determinations. For sulphur analysis a 1 mL dark sealed glass tube was used to store the samples, and immediately sealed to prevent sulphide oxidation [23]. For labile trace element concentrations the Diffusive Gradient in Thin Film (DGT) was used.

Surface soils and sediments (< 5 cm depth) samples were collected near the lakes (less than 3 m from the shore) with a plastic spatula and stored in a plastic bag. After dried at 40ºC overnight, they were desegregated (separation of roots), pulverized in an agate mortar and stored frieze-dried in polyethylene tubes for future analysis.

4. Analytical Methods
4.1. Water

DOC was determined using high temperature catalytic oxidation method as debrided in [24]. Briefly, an aliquot of 100 µL of water was injected in a vertical furnace made of quartz, filled with a catalyst of 0.5% Pt on aluminum oxide (Al_2O_3) and at 680°C. The CO_2 formed is measured in a Shimadzu TOC 5000A, and its concentration is determined by calibration curve method using potassium hydrogen phthalate solution as standard (0-100 mM).

Stable carbon isotope of DOC analysis measurements were done using the method described in [25]. Samples were analyzed using a Thermo Electron Surveyor plus HPLC System. Results are expressed as δ-values relative to the VPDB standard (Pee Dee Belemnite), and are defined as [26]:

$$\delta^{13}C(‰) = \left[\frac{\left(\frac{^{13}C}{^{12}C}\right)_{sample}}{\left(\frac{^{13}C}{^{12}C}\right)_{standard}} - 1\right] \times 1000 \quad (1)$$

The contribution of carbon from C4 plants and C3 plants were compared with literature.

The labile trace elements concentration was measured using the Diffusive Gradient in Thin films (DGT) technique described by Larner et al. (2006). The DGT samplers (DGT Research Ltd, UK) were deployed of c.a. 48h at depth to sample. Elution of metals from the Chelex binding phase was carried out by immersion in 5.0 ml of 1% (v/v) bi-distilled HNO_3. The elution extracts were then diluted with Milli-Q water (18 MΩ, Millipore) prior to ICP-MS analysis. The concentrations of Cu, Cr, Ni, Pb and Zn in the DGT's elution solution were measured by Inductively Coupled Plasma Mass Spectrometry (ICP-MS - Perkin Elmer ELAN DRC-e) using the follow isotopes: ^{63}Cu, ^{52}Cr, ^{60}Ni, ^{208}Pb, and ^{66}Zn. The quantification was made by internal standard calibration method using 10 ppb Rhodium (^{103}Rh) as internal standard prepared in the following way. Multi-element stock standard 3 solution (Perkin Elmer), ultrapure water (18 MΩ, Millipore), and bi-distillate 1% HNO_3 were used for prepared standard solutions of elements between 50 ng/L and 200 µg/L and blanks. The metals concentration (C_{DGT}) were calculated using (Larner et al. 2006):

$$C_{DGT} = C_{ICP} \times \frac{V_{HNO_3} + V_{gel}}{f_e} \times \frac{\Delta g}{D.t.A} \quad (2)$$

$C_{ICP}(\mu g/L): measured\ directly\ by\ ICP - MS$
$V_{HNO_3}: volume\ of\ acid\ added\ to\ the\ resin\ gel$
$V_{gel}: resin\ gel\ volume\ (0.15\ mL)$
$f_e: elution\ factor\ (0.8)$
$\Delta g: diffusive\ gel\ and\ filter\ thickness\ (0.78\ mm)$
$D: difusion\ coefficient\ of\ metal\ in\ the\ gel$
$t - the\ deployment\ time$
$A - exposure\ area\ (3.14\ cm^2)$

Diffusion coefficients were corrected for the field temperature as indicated in [27]. Also, total element concentrations were determined by ICP-MS technique described above for DGT.

Total dissolved sulphide in these samples was measured in a Metrohm apparatus equipped with a 693 VA processor and a 694 VA station. This model has a DME incorporated (work electrode) and both an Ag/AgCl/NaCl (36‰) standard electrode and a platinum electrode as an auxiliary. The quantification of the analyte was made using the standard addition method using 500 mg/L of $Na_2S.H_2O$ (anhydrous, Alfa product) as standard solution.

The determination of sulfate in water was made by turbidimetric method described in [28]. To an aliquot of 100-200 µL of water sample diluted in 21 mL of Milli-Q water, was added 5 mL of the conditioning reagent. To the mixture barium chloride dihydrate crystals ($BaCl_2.2H_2O$ from Merck, Germany) were added until the saturation point. The solution was mixed in a magnetic stirrer for 60 s at a constant speed. The absorbance of the suspension was determined at 400 nm using a Hitachi U-2000 spectrophotometer providing a light path of 5 cm. Concentrations of sulphate was determined by the calibration curve method using anhydrous Na_2SO_4 solution as standard (0-10 mM).

For remobilization tests 10 mL of surface water sample from each lake was added 200 µL of $K_2S_2O_8$. Oxidation of DOC was produced in an incubation camera in the presence of UV-A and UV-B for 45 min. The samples were analyzed by ICP-MS as described above, and the remobilization percentage calculated by:

$$R\ (\%) = \frac{[Total] - [Labile]}{[Labile]} \times 100 \qquad (3)$$

4.2. Soils and Sediments

An aliquot of each sample was dried at 105ºC overnight in an oven until constant weight (M_{105}). After dried the oven was bring to 450° C for 2h until constant weight (M_{450}). Sedimentary organic matter (LOI) was calculated by [28]:

$$\% LOI = \frac{M_{105} - M_{450}}{M_{105}} \times 100 \qquad (4)$$

300 mg of sample were packed into 7 mm zirconium rotors closed with Kel-F caps. High-resolution ^{13}C ssNMR spectra using magic angle (CPMAS) were recorded on a Bruker Avance 300 MHz spectrometer equipped with a 7 mm Wide Bore MAS probe operating at ^{13}C resonating frequency of 75.5 MHz [30]. The qualitative and semi-quantitative composition were obtained by cross polarization and total sideband suppression at a spinning speed of 5 kHz and a CP time of 1 ms with a ^1H 90º pulse-length of 4 µs and a recycle delay of 5 s [31]. In order to interpret the ^{13}C ssNMR results each spectrum was divided into eight shift regions, and assigned according to published studies (Cao et al. 2011). BGR samples were submitted to additional treatment to eliminate any paramagnetic material due to the low organic matter content described [32] based on hydrofluoric acid treatment.

An aliquot of each sample (200-300 mg) was submitted to X-Ray Power Diffraction analysis performed in a D8 Advance Bruker AXS θ-2θ diffractometer, with Ni-filtered Cu Kα radiation (λ = 1.5406 Å) operated at 40 kV and 40 mA. A 2θ ranging from 5 to 80º was used for experiments pattern acquisition using a scanning rate of 60º/h. A pattern fitting of samples diffractograms was carried out, with an ICDD (International Centre for Diffraction Data) software database (PDF-2).

Total elements concentrations in samples were determined by ICP-MS as described above for water samples. For the dissolution of solid matrix 200 mg were digested in closed Teflon bombs with 1 mL of *aqua regia* (bi-distilled 35% (v/v) HCl; bi-distilled 65% (v/v) HNO_3) and 6 ml of 40%

(v/v) HF on an oven at 100°C for 1h. After evaporation to dryness 6 mL of a 1:2 mixture of H_2O_2 (30% w/v; Panreac, Spain) and bi-distilled HNO_3 1% (v/v) was added. The mixture was heated at 80°C for 1h in open Teflon bombs, and after cool down carefully transferred to sample vials, diluted to 50 mL using ultrapure Milli-Q water, and refrigerated at 4°C until analysis. Certificate reference materials (CRM) were used for recovery and quality control. Multi-element stock standard 3 solution (Perkin Elmer), ultrapure water (18 MΩ, Millipore), and bi-distillate 1% HNO_3 were used for prepared standard solutions of elements between 100 ng/L and 200 µg/L and blanks. The elements concentration was calculated using:

$$C_{soil/sed} = C_{ICP} \times 50\ mL \times \frac{1}{M_{soil/sed}} \qquad (5)$$

Chromium reduced sulphur (CRS = S^0 + FeS_2) method described in [34] were used to quantify pyrite and S^0 in sediments. The Acid volatile sulphide concentration is obtained by acid attack (HCl 1M) to produced H_2S which is then trapped on NaOH 1M solution [35]. S^0 was extracted from 100 mg of dried sediment by 16h stirring with 20 mL of acetone followed by centrifugation (3000 rpm/10 min) and filtration through 0.45 µm membranes. The residue was then placed in the reaction vessel with 10 mL HCl 1M and purged with N_2 for 20 min to release AVS (reaction time of 15 min). After, 50 mL of $CrCl_3$ in 1 N HCl was added and let to react over 1h. Method recoveries were evaluated by using the same methodology with standard pyrite sample (Alfa Aesar products). Recoveries were more than 97% using this procedure. Elemental sulphur was determined using the same CRS method but in the acetone extracts. The measurements of the released H_2S were made by Differential Pulse Polarography in a Metrohm apparatus described above.

Each sediment sample was submitted to sequential extraction as debrided in [36]. An aliquot of sample (c.a. 1g) was stirred for 6h with 20 mL of $NH_2OH.HCl$ 0.04 M solution in CH_3COOH (25%). The supernatant solution was removed by centrifugation at 3000 rpm for 10 minutes and filtered in 0.45 mm membranes. The solid residue is then submitted to HCl 1M extraction, and the supernatant is collected again. Finally, to the residue H_2O_2 is added followed by UV irradiance and the supernatant collected. TEs were determined in all extracted solution by Graphite Furnace Atomic Absorption Spectrometry (Perkin Elmer AAnalyst 600).

5. Results and Discussion

5.1. Water

A systematic increase of DOC from the surface to the bottom water was observed which may be related to the diffusion of DOC from the lake sediments which has higher content of OM (see section 6.1), or from the ice cover season (formation of ice is a downward process), which accumulates DOC in the bottom. SAS 1A/2A and KWK12 had the higher values of DOC, while BGR had the lowest concentration measured. A negative spearman correlation ($r_s = -0.647$; $p<0.01$) was found between DOC (mg/L) and DO (mg/L) suggesting that OM mineralization by oxygen occur in the water column [16]. Also a decrease of DOC at the surface water can also be explained by OM photo-degradation by UV radiation. The δ^{13}C-DOC analysis showed an origin of this matter mainly been from C_3 plants (-27‰) [25]. Sulfate concentration varied in range from 0.1 to 1.2 mM with maxima at the surface in each lake. Interestingly as sulphate levels decrease with depth, an increase of dissolved sulphide was observed, suggesting that OM is also mineralized by SO_4^{2-}, producing sulphide

[28]. In fact, a negative spearman correlation was obtained (r_s=-0.941; $p<0.05$) between the two dissolved sulphur species.

Trace element vertical profiles presented a clear stratification in all lakes, with a more evidence on BGR1, possible related to the higher lake depth. Figure 2 shows the vertical profile of Cu.
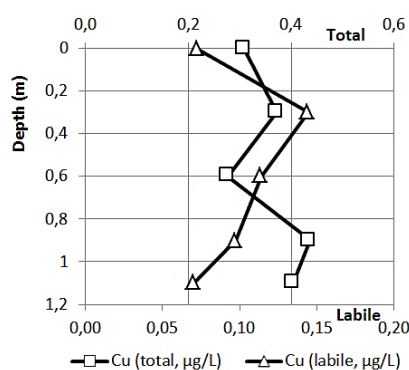

Figure 2: Labile and total concentration profiles in µg/L of copper in water column for SAS 1A.

From figure 2, it appears that at surface water OM degradation occurs leading to release of Cu to water, enhance its labile concentration. An increase of total with a decrease of labile fraction implies that new OM-Cu complexes may form [37]. At the bottom, total and labile decrease possible because of sulphide precipitation [33].

From remobilization experiment results (figure 3) an increase of labile fraction of TE was observed, more pronounced in SAS and KWK samples, with higher DOC.
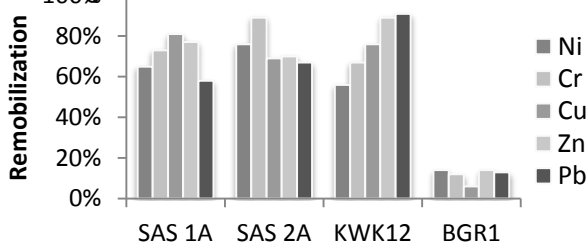

Figure 3: Trace elements remobilization (%) to water after UV treatment.

These suggest that the DOC mineralization is probably the main source of these elements in the lakes with high carbon content [16].

5.2. Soils and Sediments

With exception for BGR1 (<2%), high content in sedimentary organic matter (>63%) was determined for all sampled soils and sediments by LOI (%) method. These results suggests that OM in these lakes are related to palsas (mounds of peat containing a permafrost core of peat or silt), and lithalsas (mineral mounds) that surround the lakes [20]. From ss[13]CNMR spectra (figure 4), the higher ^{13}C signals intensity was observed for O-alkyl-C (averaged 48%) and alkyl-C (averaged 23%).
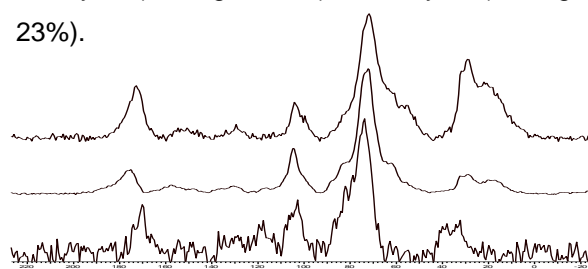

Figure 4: ^{13}C ssNMR experimental results (220-0 ppm) for soil (a) SAS 1A; (b) KWK12; (c) BGR1.

Our results suggest that OM on is mainly composed by polysaccharides and peptides as the main components, with small amounts of lignin. These compounds represent the main constitutes of plants residues, which appears to be in agreement of δ^{13}C-DOC results [31].

The mineralogical composition of soils/sediments showed the presence of SiO_2 and $NaAlSi_3O_8$, identified only on BGR samples. In fact, the other lakes showed an XPRD diffractogram pattern characteristic of amorphous matrix.

TEs enrichment was observed in BGR, and less for the lakes with higher OM content. A negative significant spearman correlation ($p<0.05$) between TEs and the LOI was observed, suggesting a reduced availability possible by complexation with humic acids and/or lignin [38]. Contrary, a positive spearman correlation ($p<0.05$) was found with aluminum and TEs suggesting that the retention of the analyzed TEs

in soils/sediments is mainly due the inorganic fraction of the soil/sediment, possible in TE-sulphide form [33].

Our results showed that inorganic-S was the major constituent (from total S) in BGR, whereas in the others lakes an opposite result was verified, which is in parallel with the OM content. Among the inorganic sulphur species, AVS was the major inorganic sulphur compound, suggesting that the sulphides present were recently formed by precipitation of FeS in the water column [39]. Finally, the sequential extraction procedure shows that TEs are mainly associated with the sulphide fraction of soils, corroborating the aluminium trend obtained.

6. Conclusion

The permafrost soils that originated the lakes play a major role in their chemistry. As an example the organic-sulphur in highly organic lakes (SAS and KWK) are the most dominant sulphur compounds and apparently have a less content on other trace elements. However, the biogeochemical processes seem to be identical in all the catchments. In all the studied lakes dissolved oxygen decrease with depth suggesting its consumption by the mineralization of the natural organic matter. This mineralization was also evidenced by a similar consumption of sulphate and the consequent production of dissolved sulphide. This process tends to reduce the concentration of DOC in the water column, which is more pronounced at the surface. This downward increase of DOC may also be related to photo-oxidation (of OM) at the surface and molecular diffusing (and possible the frozen effect) at the sediment/water interface. The DOC in the studied lakes is from plant origin (δ^{13}C-DOC data) and is also the source of labile TEs to the water column. The experiments done in the

UV-irradiation camera indicate an increase of labile TEs in solution due to the mineralization of organic matter corroborating this hypothesis.

The vertical profiles for the studied TEs showed that besides their release during OM mineralization there are also other competing process in the water column: complexation with DOC (e.g. SAS 2A) and precipitation (or co-precipitation) as metal-sulphides (e.g. Cu and Pb in SAS 1A). This precipitation was evidenced in all the studied lakes since they all present a significant amount of TEs-sulphide the topmost sediments (sequential extractions) mainly in the form of AVS (the most reactive form of reduced inorganic sulphur compounds). In spite of the role of sulphur in the retention of TEs ate the surface sediments, the associated of these elements in aluminium contained minerals (alumino-silicates) or other more refractory compound should not be excluded since a considerable amount of those TEs were not extracted by the used extractants.

The ssNMR data clearly showed that NOM is mineralized in the sediments since the metabolites of cellulose degradation were identified by this technique. In water column only indirect evidences of this mineralization process were identified (UV experiments and DO and Sulphate reduction).

7. References

[1]   Grosse, G. et al: Thermokarst lakes, drainage, and drained basins, in: Treatise on Geomorphology, edited by: Shroder, J., Giardino, R., and Harbor, J., Academic Press, San Diego, CA, vol. 8, Glacial and Periglacial Geomorphology, 325-353, 2013

[2]   Schuur E. A. G. et al. (2008) Vulnerability of permafrost carbon to climate change: implications for the global carbon cycle. Bioscience 58, pp. 701-714

[3] Lawrence D. M., Slater A. G. 2005. A projection of severe near-surface permafrost degradation during the 21st century. Geophysical Research Letters 32: L24401. DOI:10.1029/2005GL025080

[4] Hopkins D. M. 1949. Thaw lakes and thaw sinks in the Imuruk Lake area, Seward Peninsula Alaska. Journal of Geology 57, 119-131

[5] Walter K. M. et al. 2007. Thermokarst lakes as a source of atmospheric CH4 during the last deglaciation. Science 318, pp. 633-636

[6] Arp C. D. and Jones B. M. 2008. Geography of Alaska Lake Districts. U. S. Geological Survey Scientific Investigations Report, Nº 5215, pp. 1-40

[7] Morgenstern A et al. . 2011. Spatial analyses of thermokarst lakes and basins in Yedoma land scapes of the Lena Delta. The Cryosphere 5, 849–867. DOI: 10.5194/tc-5-849-2011

[8] Burn C. R. 2002. Tundra lakes and permafrost, Richards Island, western Arctic coast, Canada. Canadian Journal of Earth Sciences 39, 1281-1298

[9] Zimov S. A. et al. 1997. North Siberian lakes: a methane source fueled by pleistocene carbon. Science 277, pp. 800-802

[10] Watanabe S. et al. (2011). Optical diversity of thaw ponds in discontinuous permafrost: a model system for water color analysis. J. Geophys. Res. 116:G02003. Doi: 10.1029/2010JG001380

[11] Negandhi K. et al. 2013. Small Thaw Ponds: An Unaccounted Source of Methane in the Canadian High Arctic. PLoS ONE 8(11): e78204. doi:10.1371/journal.pone.0078204

[12] Vincent W. F. et al. 2013. Climatic Change and Global Warming of Inland Waters: Impacts and Mitigation for Ecosystems and Societies. Chap 2: Climate Impacts on Arctic Lake Ecosystems. First Edition. Edited by Charles R. Goldman, Michio Kumagai and Richard D. Robarts. Wiley & Sons, Ltd

[13] Breton J. et al. Limnological properties of permafrost thaw ponds in northeastern Canada. Can. J. Fish. Aquat. Sci. Vol. 66, 2009

[14] Sepulveda-Jauregui A. et al. 2015. Methane and carbon dioxide emissions from 40 lakes along a north–south latitudinal transect in Alaska. Biogeosciences, 12, 3197–3223, Doi: 10.5194/bg-12-3197-2015

[15] Pokrovsky O. S. et al. Biogeochemistry of organic carbon, CO2, CH4, and trace elements in thermokarst water bodies in discontinuous permafrost zones of Western Siberia. Biogeochemistry (2013) 113:573–593

[16] Audry S. et al. (2011) Organic matter mineralization and trace element post-depositional redistribution in Western Siberia thermokarst lake sediments. Biogeosciences 8:3341–3358. doi:10.5194/bg-8-3341-2011

[17] Lamarre A. et al. 2012. Holocene paleohydrological reconstruction and carbon accumulation of a permafrost peatland using testate amoeba and macrofossil analyses, Kuujjuarapik, subarctic Québec, Canada. Review of Palaeobotany and Palynology 186 pp 131–141

[18] Przytulska A. et al. 2014. Climate Effects on High Latitude Daphnia via Food Quality and Thresholds. PLoS ONE 10(5): e0126231. doi:10.1371/journal.pone.0126231

[19] Bhiry N. et al. 2011. Environmental change in the Great Whale River region, Hudson Bay: Five decades of multidisciplinary research by Centre d'études nordiques (CEN). Ecoscience 18, 182–203

[20] Gurney, S. D. 2001. Aspects of the genesis, geomorphology and terminology of palsas: perennial cryogenic mounds. Prog. Phys. Geogr. 25, 249-260. Doi: 10.1177/030913330102500205

[21] Crevecoeur S. et al. (2015) Bacterial community structure across environmental gradients in permafrost thaw ponds: methanotroph-rich ecosystems. Front. Microbiol. 6:192. Doi: 10.3389/fmicb.2015.00192

[22] Canário J., 2004. Mercúrio e monometilmercúrio na cala do norte do estuário do Tejo. Dissertação apresentada à Universidade Nova de Lisboa, Faculdade de Ciências e Tecnologia, para obtenção do grau de doutor em ciências do ambiente, pp 48

[23] Metzler D. E. Biochemistry Vol. 2. Chapt 18 Elsevier Edition. Academic Press. USA 2003

[24] Sugimura Y. and Suzuki Y. 1988. A high temperature catalytic oxidation method for the

determination of non-volatile dissolved organic carbon in seawater by direct injection of liquid sample. Mar. Chem. 24, 105-131

[25]   Brandes J. A. 2009. Rapid and precise D13C measurement of dissolved inorganic carbon in natural waters using liquid chromatography coupled to an isotope-ratio mass spectrometer. Limnol. Oceanogr.: Methods 7, 730–739

[26]   Torres M. E., Mix A. L., Rugh W. D. 2005. Precise D13C analysis of dissolved inorganic carbon in natural waters using automated headspace sampling and continuous-flow mass spectrometry. Limnol. Oceanogr.: Methods 3, pp 349–360

[27]   Zhang, H., and Davison, W. 1995. Performance Characteristics of Diffusion Gradients in Thin Films for the in Situ Measurement of Trace Metals in Aqueous Solution. Anal Chem., 67, Nº 19, 3391–3400

[28]   Rossum J. R., Villarruz P. 1961. Suggested methods for turbidimetric determination of sulphate in water. Journal of Am. Water Works Assoc. 53, pp. 873

[29   Carter M. R., and Gregorich E. G., Soil Sampling and Methods of Analysis, Canadian Society of Soil Sciente, 2th edition, CRC Press, 2008

[30]   Piccolo A. et al. 2008. Multivariate analysis of CPMAS 13C-NMR spectra of soils and humic matter as a tool to evaluate organic carbon quality in natural systems, European Journal of Soil Science, 59, pp. 496-504

[31]   Cao X. et al. 2011. Solid-state NMR analysis of soil organic matter fractions from integrated physical-chemical extraction. Soil Sci. Soc. Am. J. 75, 1374-1384

[32]   Schmidt et al. 1997. Improvement of 13C and 15N CP/MAS NMR spectra of bulk soils, particle size fractions and organic material by treatment with 10% hydrofluoric acid, European Journal of Soil Science, 48, 319-328

[33]   Lewis A., van Hille R. 2006. An exploration into the sulphide precipitation method and its effect on metal sulphide removal. Hydrometallurgy. Volume 81, Issues 3–4, March 2006, Pages 197–204

[34]   Canfield D. E. et al. 1986. The use of chromium reduction in the analysis of reduced inorganic sulfur in sediments and shales. Chemical Geology, 54, pp 149-155

[35]   Henneke E. et al. 1991. Determination of inorganic sulphur speciation with polarographic techniques: Some preliminary results for recent hypersaline anoxic sediments. In: M.B. Cita, G.J. de Lange and E. Olausson (Editors), Anoxic Basins and Sapropel Deposition in the Eastern Mediterranean: Past and Present. Mar. Geol., 100, 115-123

[36]   Tessier A. et al. Sequential extraction procedure for the speciation of particulate trace metals. Analytical Chemistry, vol. 51, no. 7, pp. 844–851

[37]   Stolpe B. et al. (2010) Size and composition of colloidal organic matter and trace elements in the Mississippi River, Pearl River and the northern Gulf of Mexico, as characterized by flow field-flow fractionation. Marine Chem 118:119–128

[38]   Cresser M. et al. Soil chemistry and its applications, Cambridge Environmental Chemistry Series 5, 1993

[39]   Rickard D. and Morse J. (2005) Acid volatile sulfide (AVS). Mar. Chem. 97, 141–197

        Larner B. L et al. Evaluation of diffusive gradients in thin film (DGT) samplers for measuring contaminants in the Antarctic marine environment. Chemosphere 65 (2006) 811-8200-802